

Oil & Natural Gas Technology

DOE Award No.: DE-NT0005669

Quarterly Report

July 1 2010 to September 30 2010

Heat Flow and Gas Hydrates on the Continental Margin of India: Building on Results from NGHP Expedition 01

Submitted by:
College of Oceanic and Atmospheric Science
Oregon State University
Corvallis, OR 97331

Principal Investigator: Anne M. Trehu

Prepared for:
United States Department of Energy
National Energy Technology Laboratory

November 10, 2010



Office of Fossil Energy

Table of Contents:	
Summary	2
Justification for modeling 1D sedimentation in the Andaman Basin	3
Porosity and Compaction	7
Modeling	9
Scenario 1	11
Scenario 2	12
Scenario 3	14
Scenario 4	15
Discussion	17
References	18
Cost Status	19
Publications, Conference Presentations and other Products	

List of Figures:	
Figure 1. Heat flow as a function of depth in the Andaman Basin	4
Figure 2. Site 17 thermal gradient	5
Figure 3. Heat flow as a function of lithospheric age	7
Figure 4. Porosity at site 17	9
Figure 5. Scenario 1 model – matching extrapolated measured sedimentation rate	11
Figure 6. Scenario 2 model – high sedimentation rate	13
Figure 7. Scenario 3 model – old lithosphere	14
Figure 8. Scenario 4 model – fitting sedimentation rate and heat flow	16

List of Tables:	
Table 1. Constants used in models	10
Table 2. Scenario 1 modeled variables – matching extrapolated measured sedimentation rate	11
Table 3. Scenario 2 modeled variables – high sedimentation rate	12
Table 4. Scenario 3 modeled variables – old lithosphere	14
Table 5. Scenario 4 modeled variables – fitting sedimentation rate and heat flow	15
Table 6. Project costing profile for Budget Period 8	

Summary

In October 2008, graduate student Peter Kannberg and Professor Anne Trehu began working on the National Energy Technology Laboratory (NETL) funded project entitled *Heat flow and gas hydrates on the continental margin of India: Building on results from NGHP expedition 01*. This project is designed to complete analysis, interpretation and modeling of downhole temperature data that were acquired in spring 2006 at 21 sites drilled in gas hydrate-bearing sediments on the continental margin of India. In addition to finding several rich gas hydrate deposits, this expedition provided a number of important new insights into the geologic conditions leading to such deposits .

Work during this quarter focused on 1 dimensional modeling of the effect of sedimentation on the temperature vs depth profile in the Andaman Sea. At this site, the temperature gradient of $19^{\circ}\text{C}/\text{km}$ is surprisingly low, leading to a very thick region in which gas hydrate is stable. High ash concentrations in this forearc environment leads to excellent gas hydrate "habitat." We examined a number of possible scenarios related to basement age and sedimentation rate in this poorly known region. Sedimentation rates based on biostratigraphic datums found during NGHP Expedition 1 are, when extrapolated over the entire sediment column, unable to recreate the anomalously low heat flow at site 17 unless the underlying lithosphere is at least 500 Ma, which is unlikely. An alternative model that reproduces the observed temperature gradient includes a period of sedimentation at a rate of 2000 cm/ky followed by a sedimentation rate of 5.7 cm/ky, as defined by the biostratigraphic datums. The 2000 cm/ky sedimentation rate needed to support such a model is typically found in deltaic environments. Whether lithologic data are compatible with such a large change in sedimentation rate is not clear; no lithologic change has been reported, but an anomalous increase in porosity at 200 m depth is compatible with this model.

The project also supports development of human resources for hydrate studies by supporting tuition for Kannberg to take courses leading to a Masters degree in oceanography and geophysics.

Justification for modeling 1D sedimentation in the Andaman basin

Heat flow in the Andaman basin is constrained by both drilling data from National Gas Hydrates Programme (NGHP) Expedition 01, site 17 and by apparent heat flow derived from Bottom Simulating Reflector (BSR) depth (Fig. 1A). Average apparent heat flow in the region determined from BSR observations at the same water depth depths is 17.0 mW/m^2 (Fig. 1B). Through multiple downhole temperature measurements, the geothermal gradient at site 17 was determined to be 19°C/km (Fig. 2A), which when multiplied by a thermal conductivity of $0.85 \text{ Wm}^{-1}\text{K}^{-1}$ results in a surface heat flow of 16.15 mW/m^2 (Collett, 2008). This in-situ measured value falls well within one standard deviation at that depth window. This very low thermal gradient leads to a very thick hydrate stability zone (HSZ). The anomalous depth of the BSR initially led to the hypothesis that this might not be a hydrate related reflection, but rather represented a lithologic change. However the seismic reflection shows a velocity slowdown at the depth of the reflection, indicative of free gas underlying hydrate, and drilling confirmed that the reflection is approximately coincident with the base of the HSZ.

Both anomalously old lithosphere and high sedimentation rates are possible explanations for the low apparent heat flow at site 17. Modeling the one dimensional effect of sedimentation on apparent heat flow allows us to test both these hypotheses. Models constructed through this process are then considered against reasonable lithospheric age and sedimentation rate constraints.

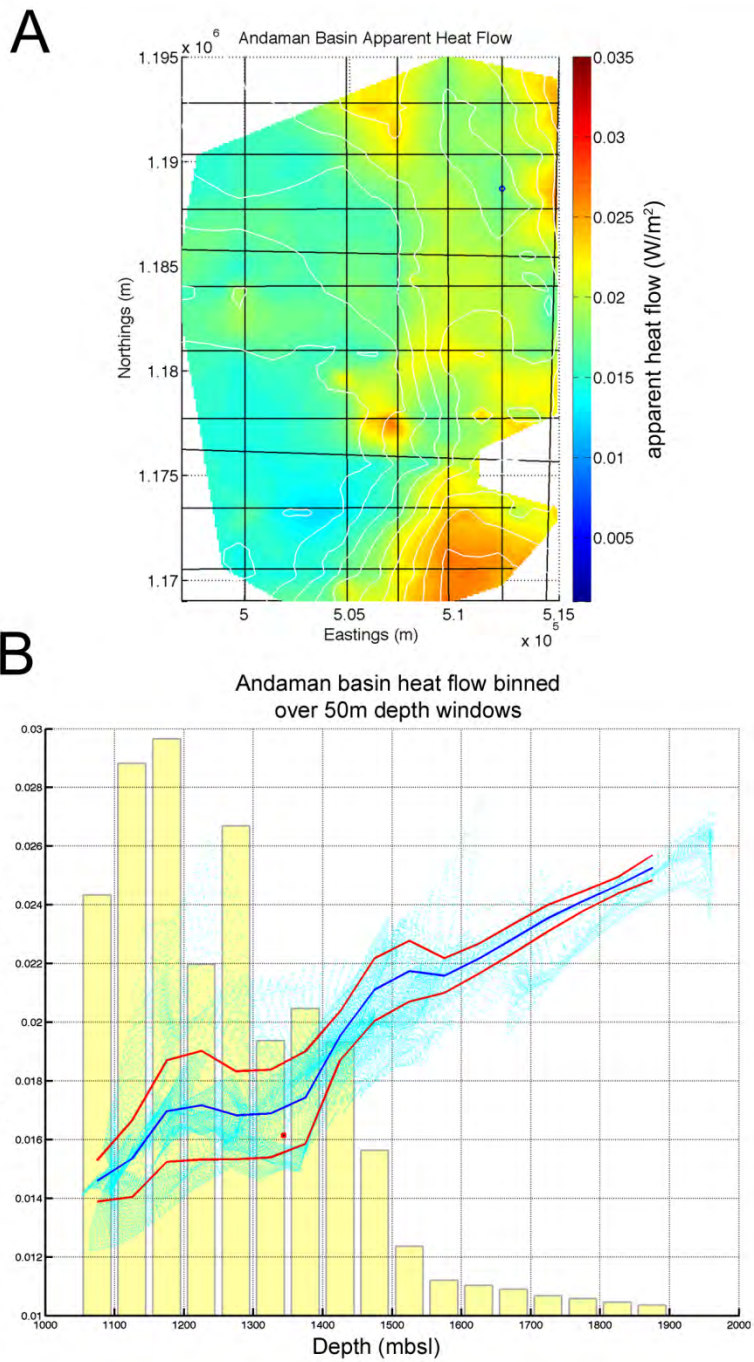


Fig. 1. Apparent heat flow as a function of depth for the Andaman Basin. A. Apparent heat flow map of the Andaman basin derived by Bottom Simulating Reflector depth. The blue circle in the northeast of the map is site 17. White lines are bathymetric contours. B. Cloud plot (cyan points) are apparent heat flow values for a 100m by 100m grid in the region encompassed in figure 1A. Overlain are average apparent heat flow values binned over 50m depth windows (blue line) showing one standard deviation (red lines). Heat flow at site 17 derived from borehole measurements (see Fig. 2) shown as single red dot. Light yellow bar graph represents the sample count for each depth bin.

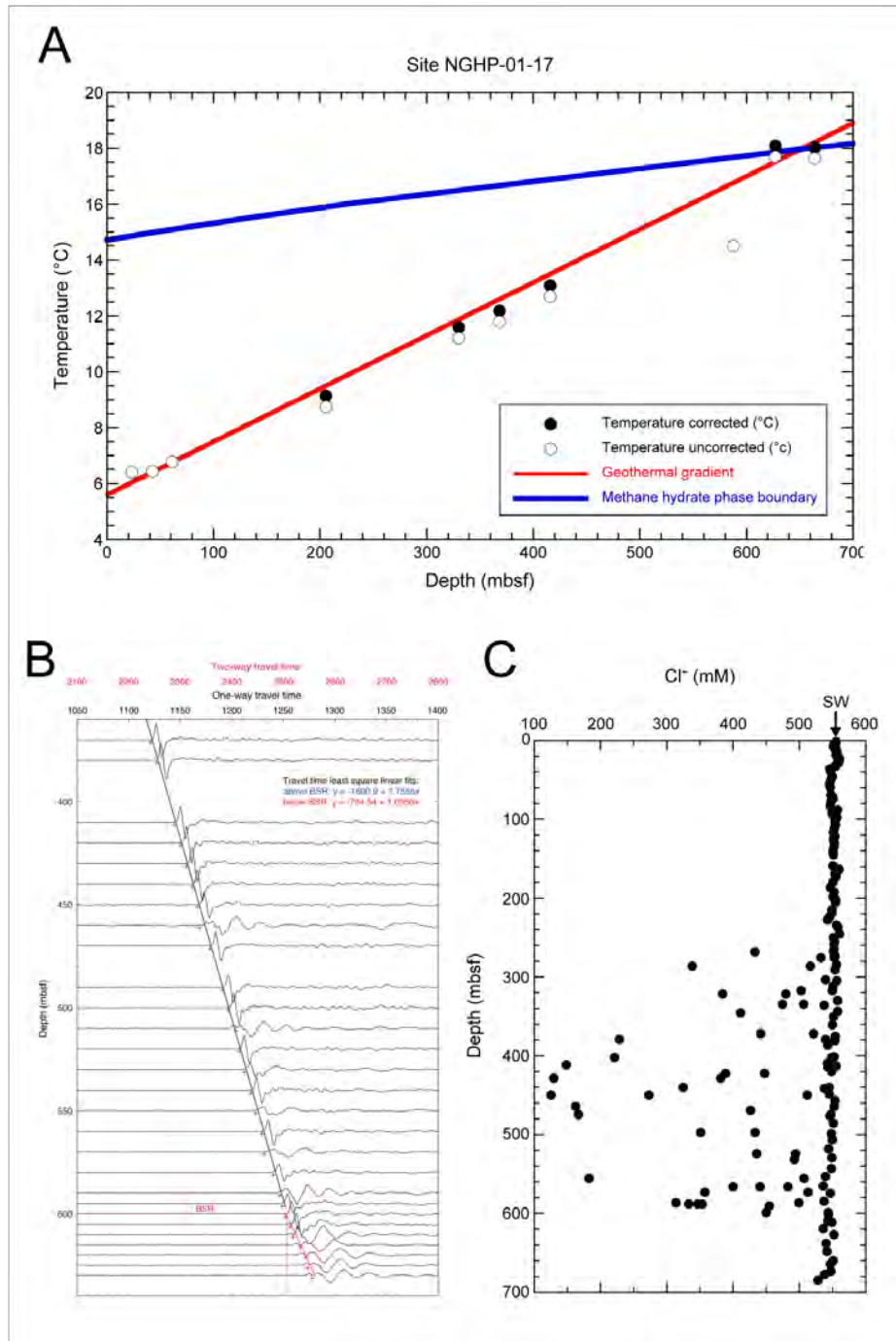


Fig. 2. A. Thermal gradient at NGHP Site 17, as determined from ADCP and DVTP borehole temperature tools. The downhole temperature increases at a rate of $19^{\circ}\text{C}/\text{km}$. Predicted depth of the gas hydrate stability boundary, assuming seawater salinity for the porewater and pure methane for the gas is ~ 650 m (from NGHP Expedition 01 Scientists, 2006). B. However, p-wave velocities determined from a vertical seismic profile (VSP) taken at the site 17 borehole indicate a shallower BSR, at 600 mbsf. C. Porewater salinity anomalies associated with the freshening effect of dissociated hydrate abruptly stop at 600 mbsf, and agree with the VSP inferred base of the hydrate stability zone.

While the geothermal gradient and hydrate stability curve define the depth of the base of the hydrate stability zone (BHSZ) to be 650 mbsf, both salinity measurements and vertical seismic profiles taken during NHGP expedition 01 indicated a shallower BHSZ (Fig. 2). We are currently exploring possible explanations for this. One possible explanation is that the thermal gradient is not linear.

Both sedimentation and erosion affect conductive heat flow. High sedimentation rates will decrease near-surface heat flow estimates while erosion exposes deeper, warmer sediments, resulting in higher near-surface heat flow estimates. Lithostratigraphic examinations of the sediment column at site 17 were used to determine sedimentation rates for the upper 23 and 108 mbsf, as those were the locations of the only two biostratigraphic markers found in the 694m borehole (Collett et al, 2008). One might expect that large fluctuations in sedimentation rate would result in varying lithology; however the sedimentology at site 17 is highly uniform, suggesting that large changes in sedimentation rate during the last 15 My are unlikely. Site 17 exhibits anomalously low heat flow and the seismic and stratigraphic data do not show evidence for major unconformities, so erosion was not modeled.

Figure 3 shows the anomalous nature of the heat flow here. As oceanic lithosphere ages, heat is lost to the ocean through conduction or advection. The overlying ocean is considered to be an infinite sink, and seafloor temperatures are kept constant. The oceanic crust heat flow decreases exponentially as a function of age (fig. 3). In the absence of sedimentation, heat flow for the 80 My old lithosphere is $\sim 50 \text{ mW/m}^2$ at 250 and is $\sim 30 \text{ mW/m}^2$ at 250 My. The oldest oceanic crust is less than 200 My. Additionally, the half-space model underestimates lithospheric heat flow at ages greater than 10 My (fig. 3). Explaining the heat flow at Site 17 as the result of lithospheric age would require very old lithosphere.

Note that regionally we observe an increase in heat flow with increasing water depth, as is seen at a number of other continental margin sites (Kannberg and Trehu, in revision). This increase in heat flow with depth is the opposite of what would be predicted by the lithosphere aging model suggesting that other processes dominate heat flow patterns here.

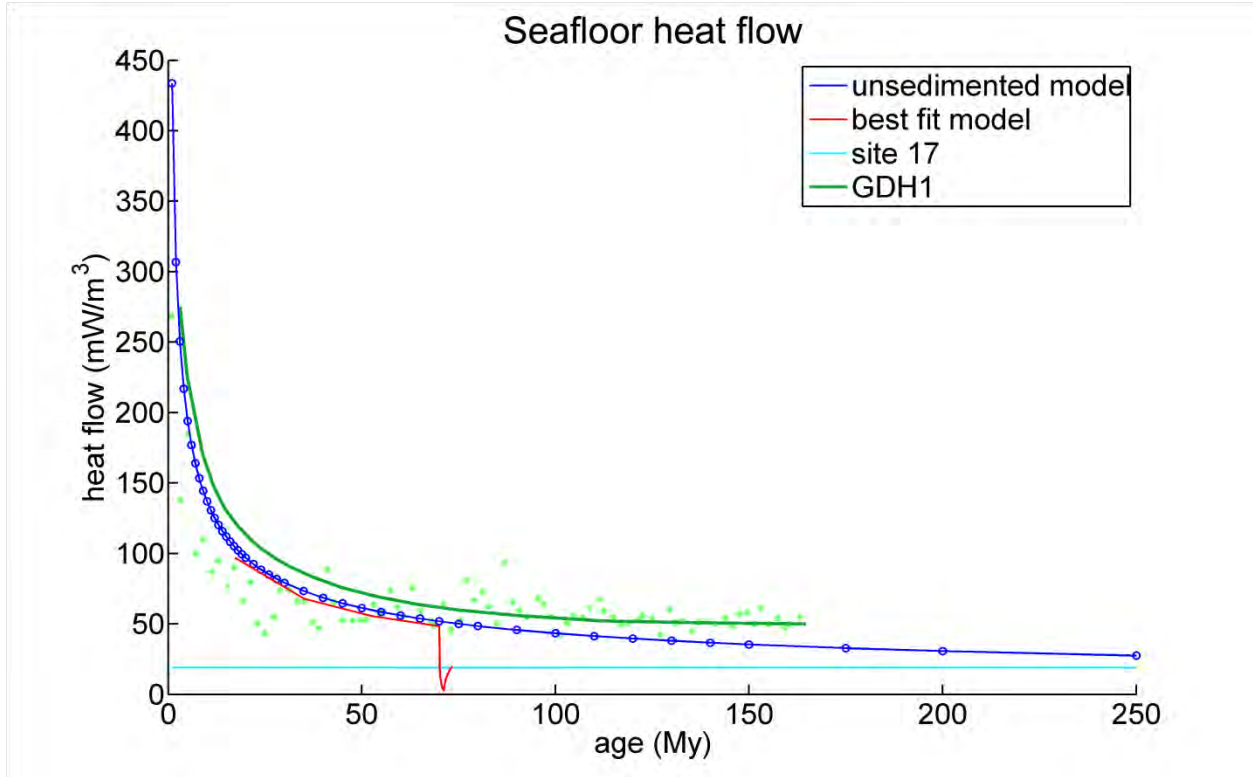


Fig. 3. Modeled heat flow for unsedimented oceanic crust as a function of lithospheric age. Open blue circles are modeled ages for which heat flow was calculated. The red line is heat flow as a function of age for the best fit model, detailed in scenario 4. The horizontal cyan line is heat flow at NGHP site 17, and shows the disparity between expected apparent heat flow and measured apparent heat flow. Light green circles are heat flow measurements binned over 2 My intervals for sites in the North Pacific and Northwest Atlantic. Dark green curve is the GDH1 model for oceanic lithosphere heat flow as a function of age (Stein and Stein 1992).

Porosity, compaction and sedimentation rate

Compaction must be taken into account when calculating sedimentation rate from biostratigraphic datums. Compaction results in a decrease in porosity with increasing depth. In the absence of major lithologic changes, the porosity versus depth profile in sediments is expected to follow an exponential curve (Hyndman and Wang, 1993, Bahr et al, 2001, Torres et al, 2004).

Porosity at the surface ($\phi_{surface}$) was calculated from NGHP site 17 drilling data. Assuming a lithologically-defined lower porosity limit of 20% the following equation was used to determine compaction (from Torres et al, 2004):

$$\phi_z = \phi_{inf} + (\phi_{surface} - \phi_{inf}) \times e^{(-z \times \phi_{depthscale})} \quad (\text{Eq. 1})$$

Where z is depth, ϕ_{inf} is the porosity at infinity, $\phi_{surface}$ is the surface porosity for which a value of 0.68 was used in all calculations, and $\phi_{depthscale}$ is the compaction coefficient, and defines the rate at which compaction takes place (fig. 4A,C).

Site 17 exhibited an unusual porosity depth profile, with the upper 200m following a steep exponential curve, under which there is an abrupt increase in porosity which remains consistently high for the remaining 500m of the borehole (fig. 4A). Initially this was thought to be the result of dissociating disseminated hydrate creating gas pockets in core samples as they equilibrated to atmospheric conditions. However this feature is also present in the in-situ logging profiles (fig. 4B). A porosity increase at depth is typical for overpressurized sediments. Overpressurization can be caused by either a high sedimentation rate or by a formation capped by an impermeable layer. Both of these scenarios would likely be associated with a lithologic change; however even though recovery at 200 mbsf was high, likely capturing any potential variation, no apparent lithologic change was noted. (Collett, 2008).

Two biostratigraphic datums have been identified at NGHP site 17. The first, at 23 mbsf indicates an age at this depth of 0.4 Ma. The other, at 108 mbsf, is aged at 2 Ma (Collett, 2008). These values result in sedimentation rates of 5.4 cm/ky and 5.75 cm/ky for each time period, respectively. Note that the dated interval falls entirely within the upper region of normal porosity increase with depth and does not help to determine whether the increase in porosity of 200 mbsf is due to a change in sedimentation rate. Radiometric dating of the many ash layers present at site 17 would provide another independent calculation of sedimentation rate and would add datums at deeper depths, though these analyses have not yet been performed.

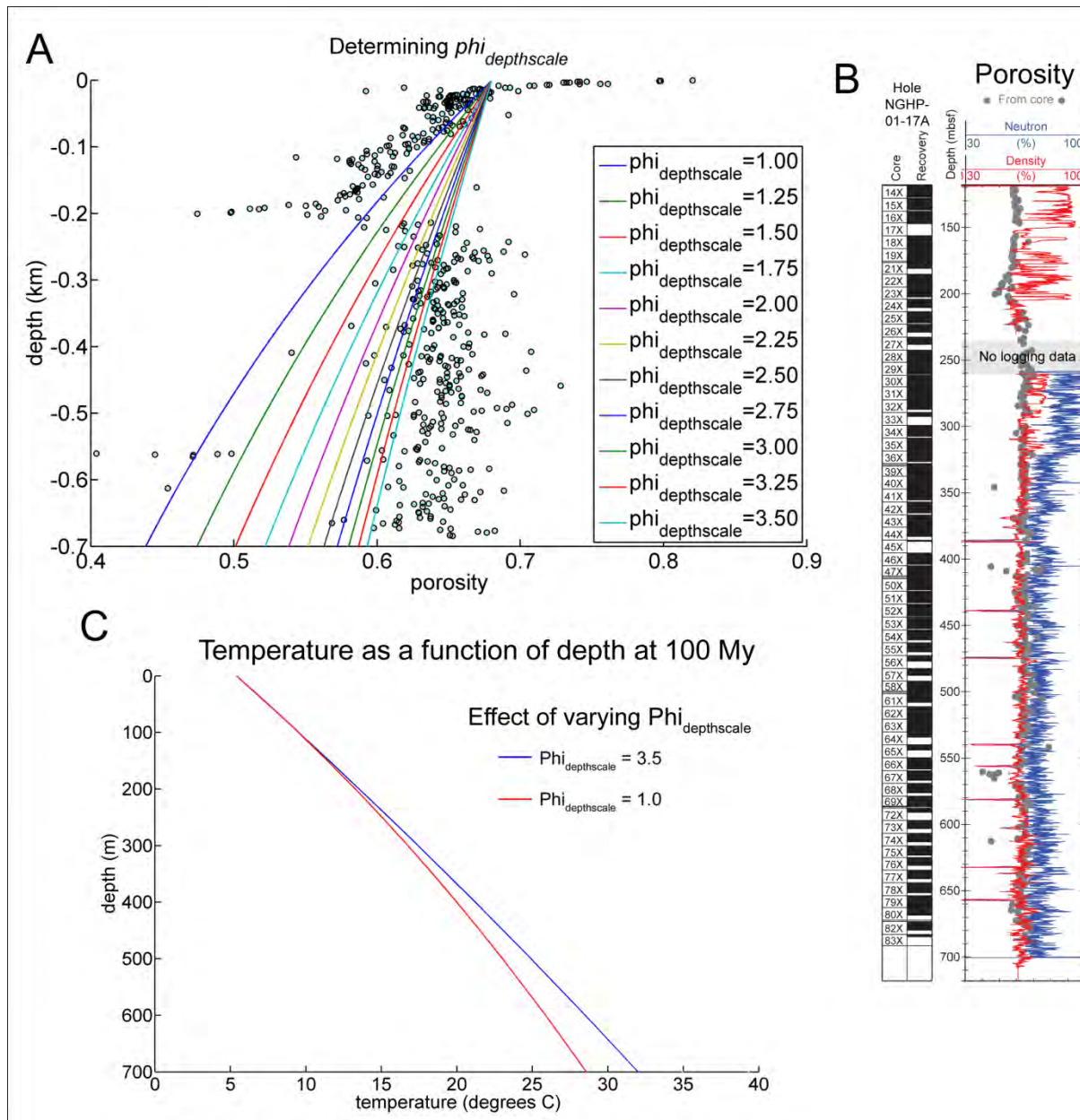


Fig. 4 Porosity at NGHP site 17. A. Shipboard porosity measurements made from core samples shown as green and black open circles. Note the abrupt change in porosity at 0.2 km depth. Multiple $\phi_{depthscale}$ plots are given to show the sensitivity of the exponential depth-porosity relationship to this term. B. Porosity measurement from downhole logging tools. Grey dots are shipboard measurements of porosity, plotted at the same scale as the logging data. Logging suggests consistently higher porosity than measurements on samples in the upper 300m of sediment, but trend similar to shipboard samples. C. Modeled temperature gradient for the upper 700 mbsf after 100 My at 5.7 cm/ky sedimentation rate for two $\phi_{depthscale}$ values, 1.0 and 3.5. A $\phi_{depthscale}$ value of 3.5 was used in all models.

Modeling:

Multiple scenarios were considered that could potentially explain the anomalously low heat flow exhibited at site 17. By varying basement age, sedimentation rate, and sediment

thickness, models were constructed in an attempt to reconstruct the anomalously low heat flow exhibited at site 17.

Model calculates heat flow and depth as a function of plate age for a specific sedimentation history. Parameters used include thermal properties of sediment, crust, and mantle, a multistage sedimentation history, compaction parameters, densities of materials, and heat generation. Constant variables used are below in table 1.

Table 1. Constant Variables	
Thermal conductivity of water	0.6 Wm ⁻¹ K ⁻¹
Thermal conductivity of sediment grains	2.74 Wm ⁻¹ K ⁻¹
Thermal conductivity of basement	2.9 Wm ⁻¹ K ⁻¹
Thermal capacity of water	4.305×10 ⁶ Jm ⁻³ K ⁻¹
Thermal capacity of sediment	2.6×10 ⁶ Jm ⁻³ K ⁻¹
Thermal capacity of basement	3.3×10 ⁶ Jm ⁻³ K ⁻¹
sediment heat generation	0.6×10 ⁻⁶ Wm ⁻³
Seafloor temperature	5.5 °C

Variables considered:

The geothermal gradient at site 17 is perhaps the best constrained variable, independently verified by BSR derived thermal gradient, and by in-situ borehole temperature measurements taken during drilling operations. The thermal gradient at site 17 is 19°C/km.

We used the two biostratigraphic datums identified at NGHP site 17 to constrain sedimentation rate. The first, at 23 mbsf indicates an age at this depth of 0.4 Ma. The other, at 108 mbsf, is aged at 2 Ma (Collett, 2008). These values result in sedimentation rates of 5.4 cm/ky and 5.75 cm/ky for each time period, respectively.

Plate age in the Andaman Basin is unknown. It is unclear whether the underlying basement is of continental or oceanic origin (Cochran, 2010). As such, there were few constraints put on this variable.

Another poorly constrained variable used in model construction is basement depth. The Andaman Basin is a relatively poorly understood region, where a basement depth of ~5000 m has been suggested by a 3D gravity inversion of the Andaman region performed by the Directorate General of Hydrocarbons of India. However, Cochran (2010) shows a seismic profile across site 17, which extend to 8 seconds of two-way travel time and does not show a basement reflection. Indicating that basement depth may be 10 km or more assuming an average sediment velocity of 2.5 km/s. It is unclear whether the basement is unresolved in the seismic reflection data because the maximum TWTT depth does not extend far enough to see the basement reflector, or whether the seismic source used was not powerful enough to resolve basement.

These variables were modeled using a program developed by Kelin Wang to model 1 dimensional effects of sedimentation on heat flow (personal communication), based on Hutchison (1985).

Scenario 1: Determining seafloor heat flow from constrained sedimentation rates and basement depth.

Scenario 1	
Variable:	value(s) used:
sediment thickness (m)	4350
plate age (My)	independent
apparent heat flow (mW/m ²)	dependent
sedimentation rate (cm/ky)	5.4-5.75

Time steps and sedimentation rates modeled	
time period (My):	sedimentation rate over time period:
0 - 0.4	5.4 cm/ky
0.4 - 2.4	5.75 cm/ky
2.4 - 6.4	5.6 cm/ky
6.4 - 21.4	5.6 cm/ky
21.4 - 141.4	5.6 cm/ky

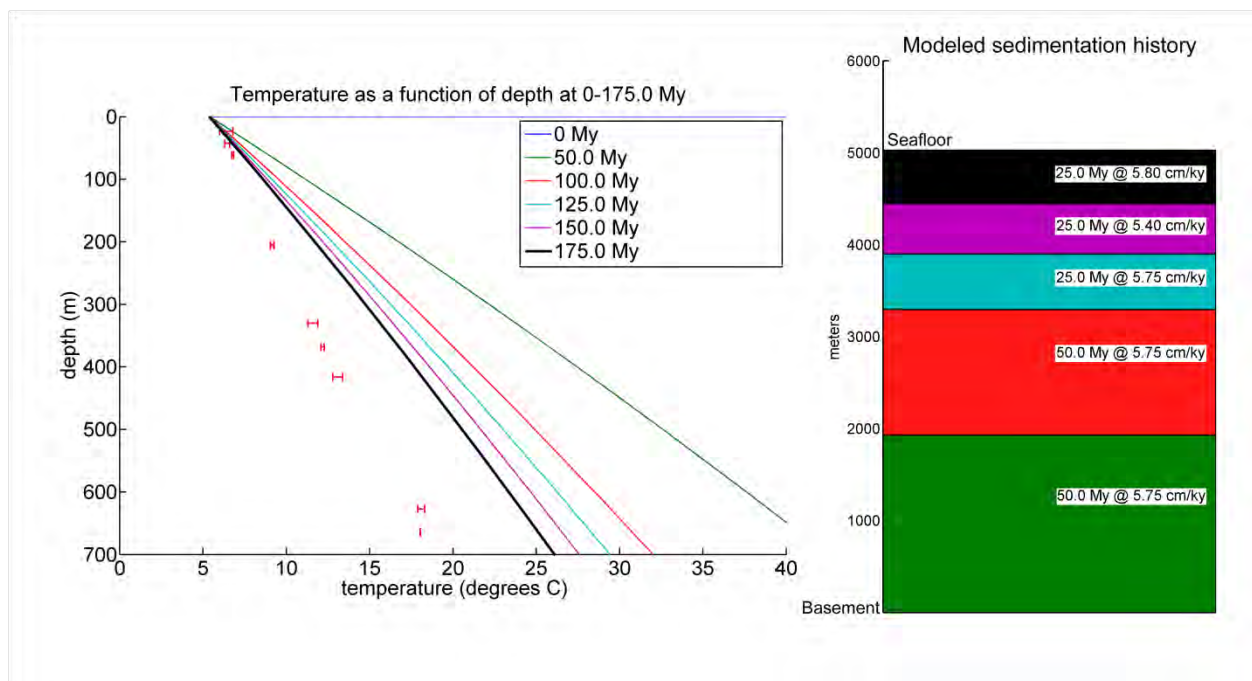


Fig 5. Results of modeling basement age and surface heat flow based on extrapolated sedimentation rates and basement depth from gravity modeling. Each curved line in 5A represents the modeled geothermal gradient at different times, each color corresponding to the color of the time period shown in the physical sedimentation history (5B). The color of the lines in 5A corresponds to the sediment profile of the same color in 5B. The red error bars indicate borehole temperature measurements and error in at site 17. This sedimentation rate and sediment thickness is incapable of producing a geothermal gradient similar to the measure gradient.

Scenario 1: In this scenario, we attempted to determine basement age by extrapolating the sedimentation rate found for upper 100mbsf to the entire sediment column and calculating heat flow as a function of basement age. This sedimentation rate, coupled with the total time period that best matched the gravity derived basement depth resulted in a plate age of 150 My, and a surface heat flow of 34mW/m². This is double the value calculated from both downhole tool measurements and BSR apparent heat flow measurements. Additional models were constructed by increasing the sedimentation rate below 700mbsf from 5.75 cm/ky to 10 cm/ky in one model and to 100cm /ky in another, while maintaining the gravityderived basement depth constraint. The 10 cm/ky model lowered basement age to 75 My and increased surface heat flow to 43 mW/m². The 100 cm/ky model lowered basement age to 19.5 My, and increased surface heat flow to 54 mW/m².

This model was unable to reproduce the apparent heat flow exhibited at site 17. We therefore tested models with both increased sedimentation rates (scenario 2) and increased basement age (scenario 3) and relaxed the constraint on total sediment thickness to determine a class of models that could produce geothermal gradients similar to those at site 17.

Scenario 2: Fitting sedimentation rate to known heat flow and basement depth.

Scenario 2		Time steps and sedimentation rates modeled	
Variable:	High sedimentation rate value(s) used:	time period (My)	sedimentation rate over time period
sediment thickness (m)	4350	0 - 0.15	1200 cm/ky
plate age (My)	dependent	0.15 - 0.3	1200 cm/ky
apparent heat flow (mW/m ²)	17	0.3 - 0.45	1200 cm/ky
sedimentation rate	independent	0.45 - 10.45	5.6 cm/ky
		10.45 - 70.45	5.6 cm/ky

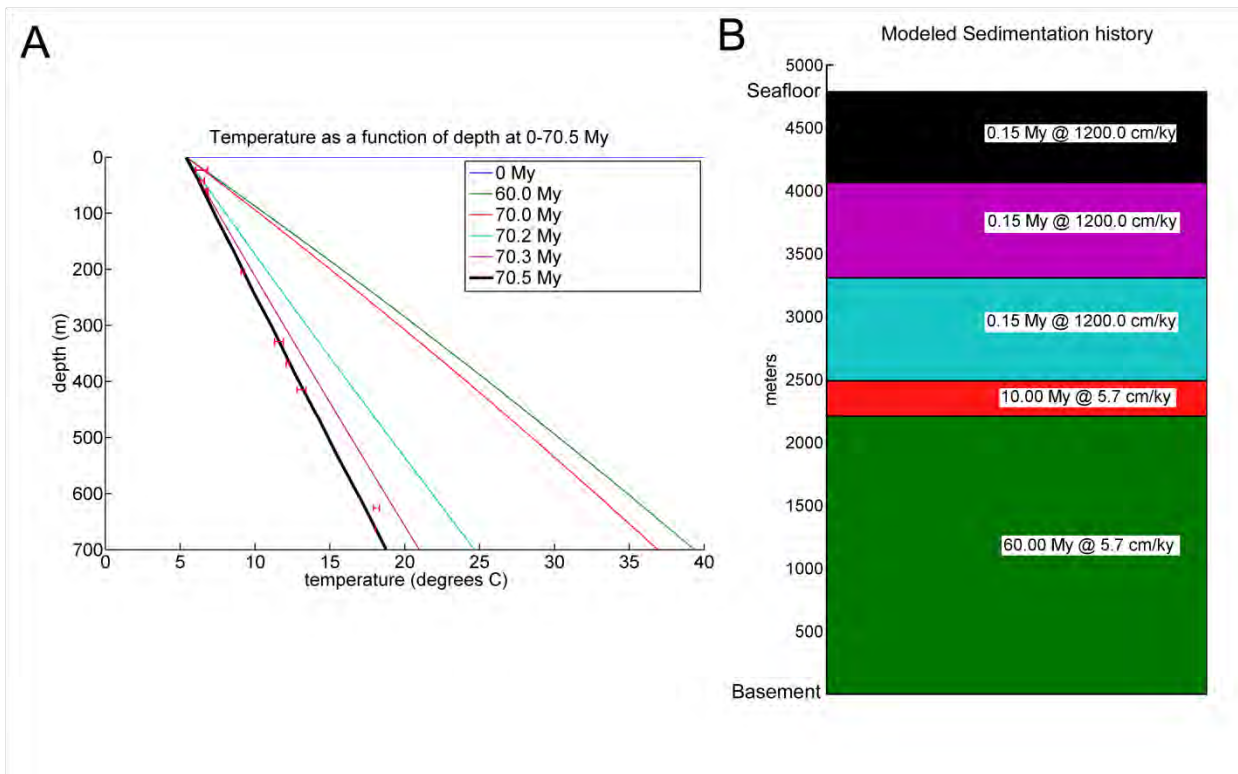


Fig 6. Results of modeling a very rapid sedimentation rate for the most recent time period, constraining thermal gradient to $19^{\circ}\text{C}/\text{km}$ and sediment thickness. A. The resulting thermal gradient for the upper 700 mbsf is plotted for each time period. Time periods are illustrated by the sedimentation history model (6B). The colored lines correspond to the colors of the sediment history. The red error bars are the individual temperature measurements and error corresponding to each measurement.

Scenario 2: In areas of high sedimentation rates, lower than expected values of surface heat flow are found. If sediment thickness is constrained by the gravity data, a sedimentation rate for the last 450,000 years would need to be 1200 cm/ky in order to depress surface heat flow values to values similar as are found at site 17. This sedimentation rate is 200 times the rate determined for the upper 108 mbsf at site 17. Additionally, high sedimentation rates for shorter periods of time, i.e. 150 ky and 300 ky (cyan and purple lines in 6A, respectively) were not sufficiently long enough to perturb the surface heat flow enough to match heat flow at site 17.

Scenario 3: Fitting basement age to measured apparent heat flow.

Scenario 3		Time steps and sedimentation rates modeled	
Variable:	Old plate	time period (My)	sedimentation rate over time period
sediment thickness (m)	value(s) used: 4350	0 - 100	1.5 cm/ky
plate age (My)	Independent variable	100 - 200	1.5 cm/ky
apparent heat flow (mW/m^2)	17	200 - 300	1.5 cm/ky
sedimentation rate	Dependent variable	300 - 400	1.5 cm/ky
		400 - 500	1.5 cm/ky

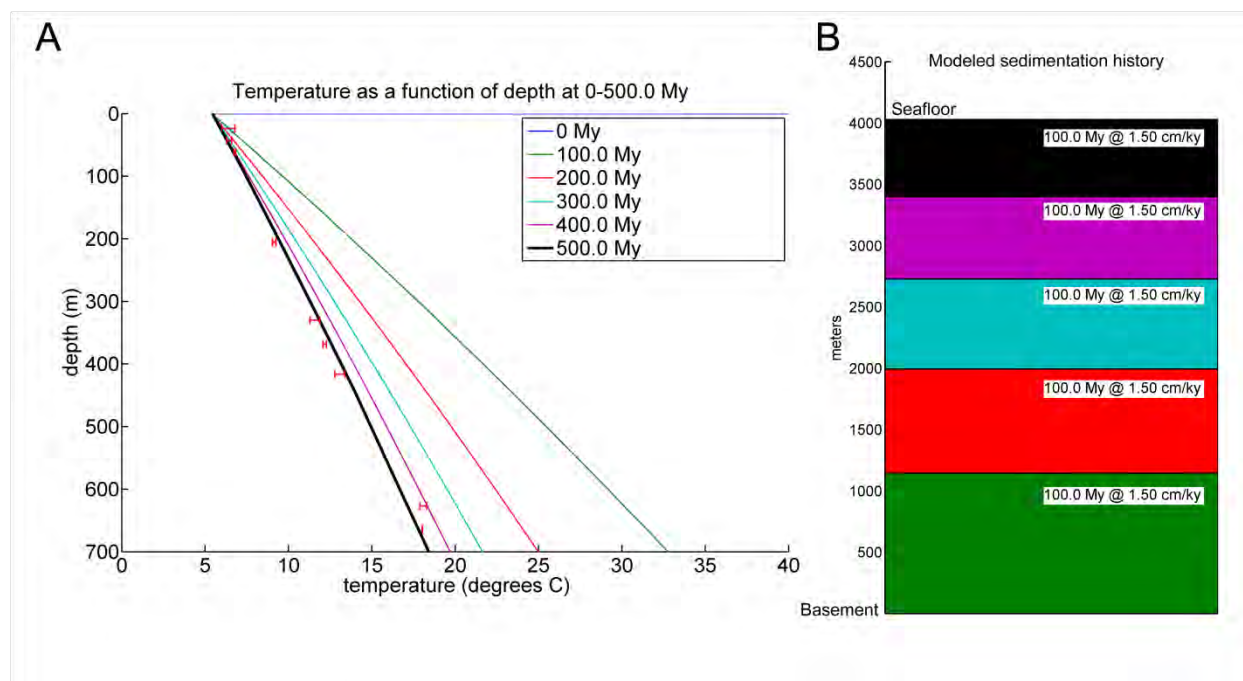


Fig 7. Results of modeling unconstrained basement age and sedimentation rate by constraining thermal gradient to $19^{\circ}C/km$ and sediment thickness to the gravity measured value. A. The resulting thermal gradient for the upper 700 mbsf is plotted for each time period. Time periods are illustrated by the sedimentation history model (7B). The colored lines correspond to the colors of the sediment history. The red error bars are the individual temperature measurements and error corresponding to each measurement.

Scenario 3: The other possible explanation of low heat flow at site 17 modeled here is very old underlying oceanic crust. In order to maintain a basement depth of ~ 4000 mbsf,

sedimentation rate must be lowered as basement age is increased. Modeling this tradeoff for basement age of 500 My, the sedimentation rate must be 1.5cm/ky. This sedimentation rate is typical of an abyssal plain environment (Kuenen, 1946). This model needs oceanic lithosphere twice the age of the oldest oceanic lithosphere on Earth (280 My old in the Mediterranean; see http://www.ngdc.noaa.gov/mgg/ocean_age/data/2008/image/age_ageerror.pdf) . We consider this model to be an unlikely explanation for the anomalously low heat flow values in the Andaman basin unless the underlying lithosphere is continental in origin. If basement is continental, a crustal thinning event long ago is needed. A seismic reflection identified as continental Moho was found in the nearby Simeulue forearc basin(Singh et al. 2008), suggesting that very old lithosphere of continental origin may be responsible for the low heat flow.

Scenario 4: Preferred model

Scenario 4		Time steps and sedimentation rates modeled	
variable	High sedimentation rate underlying low sedimentation rate	time period (My)	sedimentation rate over time period
variable	value(s) used	0 - 2	5.7 cm/ky
sediment thickness (m)	Dependent variable	2 - 2.4	2000 cm/ky
plate age (My)	Dependent variable	2.4 - 2.8	2000 cm/ky
apparent heat flow (mW/m ²)	17	2.8 - 3.2	2000 cm/ky
sedimentation rate (cm/ky)	constrained in shallowest 100m, assumed at greater depths	3.2 - 73.2	5.7 cm/ky

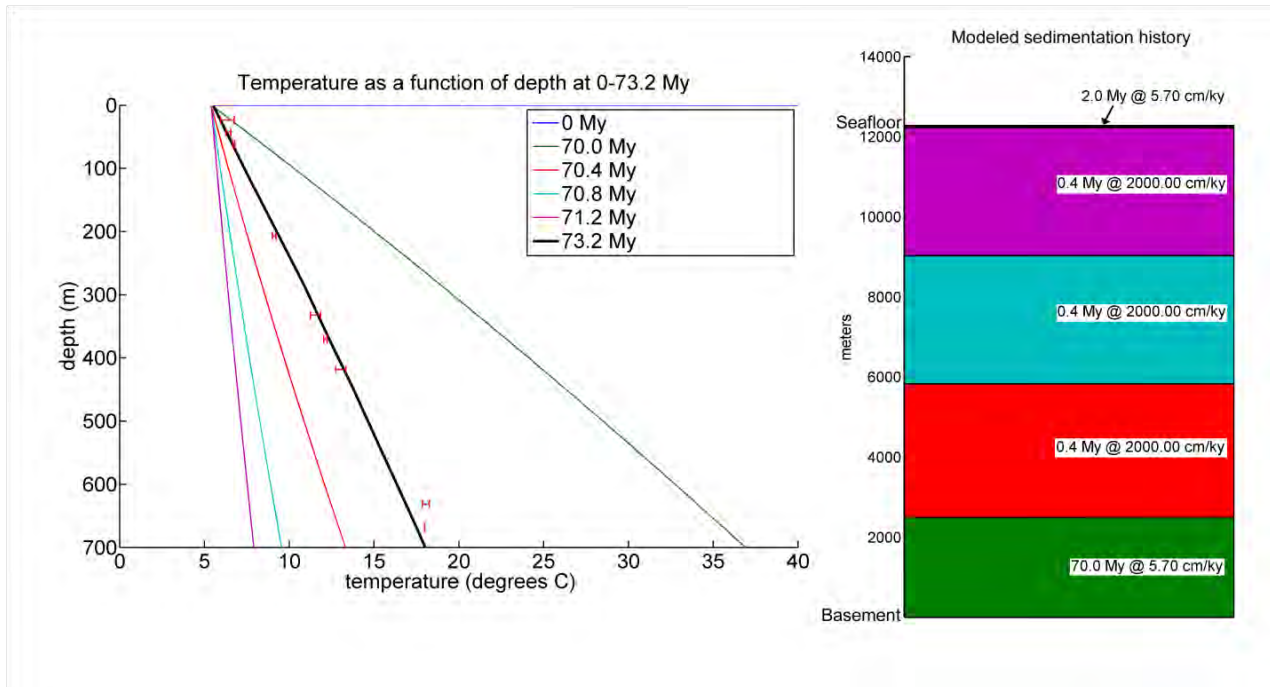


Fig. 8. Results of modeling unconstrained basement age and sediment thickness, constraining thermal gradient to $19^{\circ}\text{C}/\text{km}$ and sedimentation rate to measured values in the upper 100 mbsf, and assumed values at greater depths. A. The resulting thermal gradient for the upper 700 mbsf is plotted for each time period. Time periods are illustrated by the sedimentation history model (8B). The colored lines correspond to the colors of the sediment history. The red error bars are the individual temperature measurements and error corresponding to each measurement. An intermediate geothermal gradient of $3^{\circ}\text{C}/\text{km}$ (purple line in 5A) is needed before the final 2 My, 5.7cm/ky time step drops the thermal gradient back to measured values, at $19^{\circ}\text{C}/\text{km}$.

Scenario 4: This model attempted to reconcile the low sedimentation rate measured for the upper 108 mbsf with the much higher sedimentation rates needed to reproduce the measured geothermal gradient. This model ignored any constraints on basement age and sediment thickness, as these are the two variables that are least constrained. Additionally, sedimentation rate at depth below the lowest biostratigraphic datum at 108 mbsf are unknown. In order to achieve a final geothermal gradient after a relatively low sedimentation rate of 5.7cm/ky for 2 My, the prior high sedimentation rate time period must overshoot the measured thermal gradient. In order to achieve this overshoot, a much higher sedimentation rate and longer time period is needed relative to the high sedimentation rate model in scenario 2. Modeled is an initial period of 5.7cm/ky sedimentation rate for 70 My. The sedimentation rate for this time period is arbitrary, what is more important is that this initial period must result in old lithosphere that will produce a relatively low heat flow that will be further perturbed by a very high sedimentation rate for a short period of time. In this case 2000 cm/ky over three consecutive 0.4 My time periods. The progressively increasing overshoot is shown in figure 8A as the red, cyan, and purple lines, respectively. As the sedimentation rate is lowered to measured values to satisfy the biostratigraphic constraints of the upper 108mbsf, the apparent heat flow will begin to return to expected values for 73 My old lithosphere. After 2 My of sedimentation at a rate of 5.7 cm/ky, the thickness of this section is 108m, and the geothermal gradient is $19^{\circ}\text{C}/\text{km}$, matching the measured value at site 17.

Discussion:

The sedimentation rate of ~ 2000 cm/ky that reproduces the low geothermal gradient observed at site 17 is not commonly found in deep marine environments, but rates of this order of magnitude are found in deltaic environments (Hart et al. 1998). An inferred 4.3 km thick section of the Bengal delta was found to have a sedimentation rate of 120 cm/ky, an order of magnitude less than what is needed to produce such low thermal gradients as found in the Andaman Basin (Worm et al. 1998). One might expect that the dramatic change in sedimentation rate at 2 My in scenario 4 would result in a strong lithological in the sediment record at site 17. Although no such lithologic change was reported, the porosity profile at Site 17 is indeed suggestive of a change in sedimentation rate at approximately this time. We thus conclude that extremely rapid sedimentation from about 3-2 Ma is the most likely explanation for the very low temperature gradient observed and Site 17.

An alternative explanation could be that advective processes are mining the heat below where we are able to constrain heat flow. This process would produce a region of higher heat flow and would shoal the BSR where this advective flow crosses it. While apparent heat flow maps of the region encompassing NGHP site 17 constructed previously show increasing apparent heat flow with increasing depth, apparent heat flow never approaches the expected heat flow. However, site 17 is near the edge of where BSRs are present, and if such an anomaly is present, it could be beyond the lateral extent of this study.

With each unconstrained variable, there exists a range of solutions that will satisfy the constrained variables. The next quarter will be spent further bracketing the range of possible models, as well as interpreting these models in collaboration with NGHP 01 sedimentologists, and concatenating the results into a manuscript for publication.

References:

- Bahr D.B., E. Hutton, J. Syvitski, L. Pratson, (2001), Exponential approximations to compacted sediment porosity profiles, *Computers and Geosciences*, 27, 691-700(10)
- Cochran, J. R. (2010), Morphology and tectonics of the Andaman Forearc, northeastern Indian Ocean. *Geophysical Journal International*, 182: 631–651.
- Collett TS, Riedel M, Cochran J, Boswell R, Presley J, Kumar P, Sathe A, Lall M, Sibal V, and the NGHP Expedition 01 Scientists (2008), National Gas Hydrate Program Expedition 01 initial report, Dir. Gen. of Hydrocarbons, Minist. of Pet. and Nat. Gas, New Delhi.
- Hart, B.S., Hamilton, T.S. & Barrie, J.V., (1998) Sedimentation rates and patterns on a deep-water delta (Fraser Delta, Canada); integration of high-resolution seismic stratigraphy, core lithofacies, and 137 Cs fallout stratigraphy. *Journal of Sedimentary Research*, 68(4), 556-568.
- Hutchison, I., 1985. The effects of sedimentation and compaction on oceanic heat flow. *Geophysical Journal of the Royal Astronomical Society*, 82(3), 439-459.
- Hyndman, R.D., K. Wang, T. Yuan, G.D. Spence, (1993), Tectonic Sediment Thickening, Fluid Expulsion, and the Thermal Regime of Subduction Zone Accretionary Prisms: The Cascadia Margin off Vancouver Island, *J. Geophys. Res.*, 98, B12 21865-21876.
- Kuenen, P.K., (1946), Rate and mass of deep-sea sedimentation, *American Journal of Science*, 244(8):563-572
- Singh, S.C. et al., 2008. Seismic evidence for broken oceanic crust in the 2004 Sumatra earthquake epicentral region. *Nature Geosci*, 1(11), 777-781.
- Stein, C.A. & Stein, S., 1992. A model for the global variation in oceanic depth and heat flow with lithospheric age. *Nature*, 359(6391), 123-129.
- Torres, M.E., K. Wallman, A.M. Trehu, G. Bohrmann, W.S. Borowski, H. Tomaru, (2004), Gas hydrate growth, methane transport, and chloride enrichment at the southern summit of Hydrate Ridge, Cascadia margin off Oregon, *Earth and Planetary Science Letters* Vol. 226: 225-241.
- Worm, H. et al., 1998. Large sedimentation rate in the Bengal delta: Magnetostratigraphic dating of Cenozoic sediments from northeastern Bangladesh. *Geology*, 26(6), 487 -490.

Table 6. Project costing profile for Budget Period 8.

	July (planned)	July (actual)	August (planned)	August (actual)	September (planned)	September (actual)
PI salary & fringe benefits	1,627	522	1,627	522	1,627	522
GRA salary & fringe benefits	2,271	2,192	2,271	2,192	2,271	2,201
Computer subscription	250	0	250	0	250	750
Travel and supplies		0		0		0
Tuition	0	0	0	0	0	0
Indirect Costs	1,908	1,246	1,908	1,246	1,908	1,592
	6,056	3,960	6,056	3,960	6,056	5,065

PUBLICATIONS, CONFERENCE PRESENTATIONS AND OTHER PRODUCTS:

No publications, conference presentations or other products related to this project were produced during this quarter. A publication submitted to Marine Geophysical Research in June 2010 (budget period 7) was received and revisions were begun.

National Energy Technology Laboratory

626 Cochrans Mill Road
P.O. Box 10940
Pittsburgh, PA 15236-0940

3610 Collins Ferry Road
P.O. Box 880
Morgantown, WV 26507-0880

One West Third Street, Suite 1400
Tulsa, OK 74103-3519

1450 Queen Avenue SW
Albany, OR 97321-2198

2175 University Ave. South
Suite 201
Fairbanks, AK 99709

Visit the NETL website at:
www.netl.doe.gov

Customer Service:
1-800-553-7681

